U.S. DEPARTMENT OF COMMERCE
National Technical Information Service
PB-288 584

Characterization of Solid Residues from Fluidized-Bed Combustion Units

Tennessee Valley Authority, Chattanooga Office of Power

Prepared for

Industrial Environmental Research Lab, Research Triangle Park, NC

Jul 78

PB 288584

TVA
EPA

Tennessee Valley Authority
Energy Research Office of Power Chattanooga TN 37401
TVA PRS-31

US Environmental Protection Agency Office of Research and Development
Industrial Environmental Research Laboratory Research Triangle Park NC 27711
EPA-600/7-78-135 July 1978

Characterization of Solid Residues from Fluidized-bed Combustion Units

Interagency Energy/Environment R&D Program Report

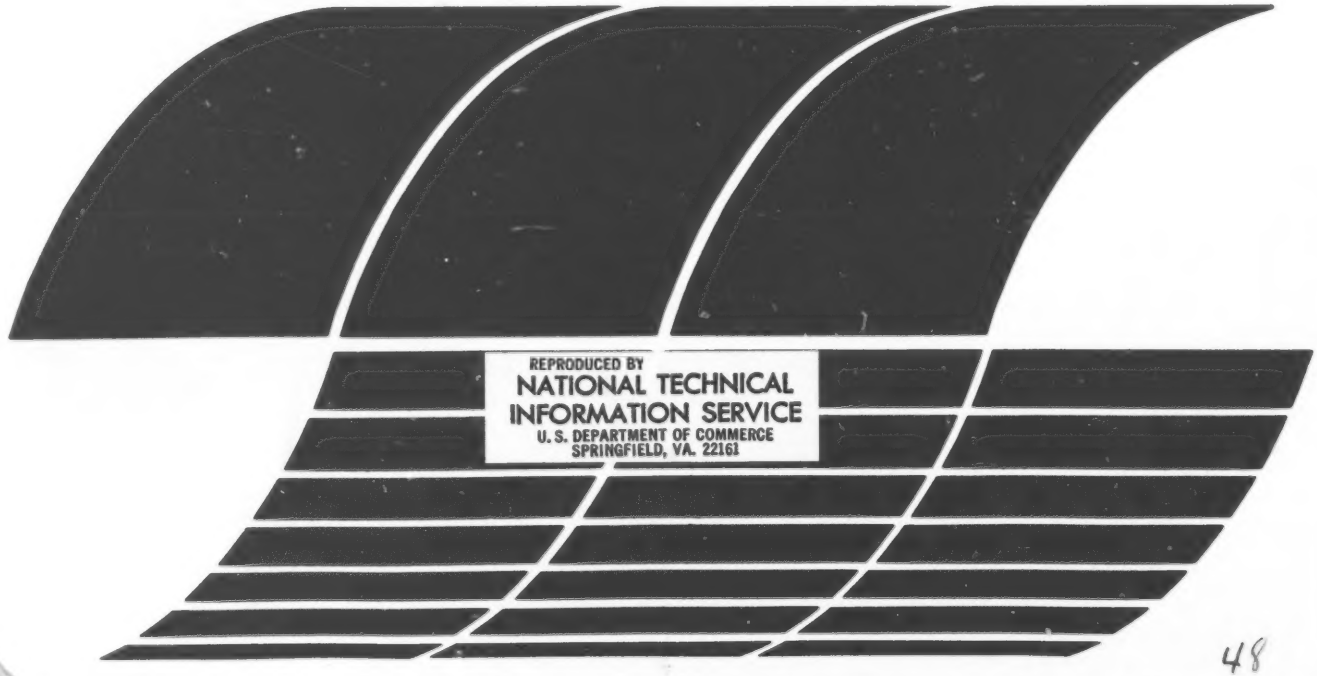

REPRODUCED BY
NATIONAL TECHNICAL INFORMATION SERVICE
U.S. DEPARTMENT OF COMMERCE
SPRINGFIELD, VA. 22161

48

RESEARCH REPORTING SERIES

Research reports of the Office of Research and Development, U.S. Environmental Protection Agency, have been grouped into nine series. These nine broad categories were established to facilitate further development and application of environmental technology. Elimination of traditional grouping was consciously planned to foster technology transfer and a maximum interface in related fields. The nine series are:

1. Environmental Health Effects Research
2. Environmental Protection Technology
3. Ecological Research
4. Environmental Monitoring
5. Socioeconomic Environmental Studies
6. Scientific and Technical Assessment Reports (STAR)
7. Interagency Energy-Environment Research and Development
8. "Special" Reports
9. Miscellaneous Reports

This report has been assigned to the INTERAGENCY ENERGY-ENVIRONMENT RESEARCH AND DEVELOPMENT series. Reports in this series result from the effort funded under the 17-agency Federal Energy/Environment Research and Development Program. These studies relate to EPA's mission to protect the public health and welfare from adverse effects of pollutants associated with energy systems. The goal of the Program is to assure the rapid development of domestic energy supplies in an environmentally-compatible manner by providing the necessary environmental data and control technology. Investigations include analyses of the transport of energy-related pollutants and their health and ecological effects; assessments of, and development of, control technologies for energy systems; and integrated assessments of a wide range of energy-related environmental issues.

EPA REVIEW NOTICE

This report has been reviewed by the participating Federal Agencies, and approved for publication. Approval does not signify that the contents necessarily reflect the views and policies of the Government, nor does mention of trade names or commercial products constitute endorsement or recommendation for use.

This document is available to the public through the National Technical Information Service, Springfield, Virginia 22161.

TECHNICAL REPORT DATA
(Please read Instructions on the reverse before completing)

1. REPORT NO. EPA-600/7-78-135	2.
3. RECIPIENT'S ACCESSION NO. PB288584	
4. TITLE AND SUBTITLE Characterization of Solid Residues from Fluidized-bed Combustion Units	5. REPORT DATE July 1978
	6. PERFORMING ORGANIZATION CODE
7. AUTHOR(S) James L. Crowe (TVA/Chattanooga) and Stephen K. Seale (TVA/Muscle Shoals)	8. PERFORMING ORGANIZATION REPORT NO. PRS-31
9. PERFORMING ORGANIZATION NAME AND ADDRESS Office of Power, TVA, Chattanooga TN 37401; and Office of Agricultural and Chemical Development, TVA, Muscle Shoals AL 35660	10. PROGRAM ELEMENT NO. EHE623A
	11. CONTRACT/GRANT NO. IAG-D7-E721
12. SPONSORING AGENCY NAME AND ADDRESS EPA, Office of Research and Development Industrial Environmental Research Laboratory Research Triangle Park, NC 27711	13. TYPE OF REPORT AND PERIOD COVERED Final; 7/75-6/77
	14. SPONSORING AGENCY CODE EPA/600/13

15. SUPPLEMENTARY NOTES IERL-RTP project officer is D. B. Henschel, Mail Drop 61, 919/541-2825. TVA project officer is J. L. Crowe.

16. ABSTRACT The report gives results of physical and chemical characterizations of samples of spent bed material and of flyash (carryover elutriated from the bed) from three experimental atmospheric and pressurized fluidized-bed combustion (FBC) units. It also gives results of characterization of samples of bed material which had been subjected to sorbent regeneration. In general, it was found that the granular material consists of three shells or zones. The outer zone, primarily $CaSO_4$, is 2-25 microns thick; an intermediate zone, $CaSO_4$ and soft-burned CaO, is 60-150 microns thick; and the third zone, in the center of the particle (for samples with incomplete sulfation), is primarily original absorbent. Particle size analysis shows that, in general, $CaSO_4$ and $Ca(OH)_2$ concentration increases as the size of the particle decreases and that $CaCO_3$ is more concentrated in the larger fraction. The FBC residue was found to stabilize sludges produced by wet lime/limestone scrubber systems so that they would not soften when contacting water.

micrometers

17. KEY WORDS AND DOCUMENT ANALYSIS

a. DESCRIPTORS		b. IDENTIFIERS/OPEN ENDED TERMS	c. COSATI Field/Group	
Pollution	Fly Ash	Pollution Control	13B	21B
Fluidized Bed	Sulfation	Stationary Sources		07C
Processing	Sorbents	Characterization	13H, 07A	11G
Solids	Sludge		07D	
Residues	Scrubbers			13I
Analyzing	Calcium Oxides		14B	07B
Properties	Calcium Carbonates			

18. DISTRIBUTION STATEMENT Unlimited	19. SECURITY CLASS *(This Report)* Unclassified	21. NO. OF PAGES 46
	20. SECURITY CLASS *(This page)* Unclassified	22. PRICE MF A01 PC A03

EPA Form 2220-1 (9-73)

PRS - 31
EPA-600/7-78-135
July 1978

Characterization of Solid Residues from Fluidized-bed Combustion Units

by

James L. Crowe

Office of Power
Tennessee Valley Authority
Chattanooga, Tennessee 37401

and

Stephen K. Seale

Office of Agricultural and Chemical Development
Tennessee Valley Authority
Muscle Shoals, Alabama 35660

EPA Interagency Agreement No. IAG-D7-E721
Program Element No. EHE623A

Project Officers: D. Bruce Henschel (EPA) and James L. Crowe (TVA)

Industrial Environmental Research Laboratory
Office of Energy, Minerals, and Industry
Research Triangle Park, NC 27711

Prepared for

U.S. ENVIRONMENTAL PROTECTION AGENCY
Office of Research and Development
Washington, DC 20460

and

Tennessee Valley Authority
Office of Power
Chattanooga, TN 37401

ABSTRACT

This report summarizes work completed during the period July 1, 1975, to June 30, 1977. The purpose of this study was to provide comprehensive chemical and physical characterization of fluidized bed combustion materials with emphasis on beneficiation and/or disposal of these materials.

Fluidized bed combustion materials were obtained from the Argonne National Laboratory, the Combustion Power Company, and the Exxon Research and Engineering Company. Samples of regenerated bed materials from Argonne National Laboratory were also characterized.

In general, granular bed material consists of three zones. The outer zone consists primarily of $CaSO_4$ and ranges in thickness from 2 to 25 microns, a center zone 60 to 150 microns consists of $CaSO_4$ and soft-burned CaO, and a third zone (in samples with incomplete sulfation) consists primarily of original absorbent.

Particle size analysis shows that in general, $CaSO_4$ and $Ca(OH)_2$ concentration increases as the size of the particle decreases and that $CaCO_3$ is more concentrated in the larger particles.

The fluidized bed combustion residue was found to stabilize sludges produced by wet lime/limestone scrubber systems such that they would not reslime upon contact with water.

CONTENTS

Abstract iii

Figures v

Tables vi

Section

1. Introduction 1

2. Conclusions 2

3. Instrumental Techniques of Characterization 4

4. Solids Characterization 5

5. Size Classification and X-ray Studies 12

6. Fluidized Bed Material--Sludge Stabilization Tests 14

FIGURES

Figure		Page
1.	Scanning electron micrographs for Combustion Power Corporation sample 20 LP	24
2.	Optical photomicrographs for Argonne samples LST-1 and LST-4	26
3.	Scanning electron micrographs for Argonne samples LST-1 and LST-4	28
4.	Optical photomicrographs for Argonne samples CCS-10 and RGL-10	30
5.	Scanning electron micrographs for Argonne samples CCS-10 and RGL-10	32
6.	Scanning electron micrographs and x-ray maps for Exxon samples 30.1, 30.2, and 32.0	34
7.	Sieve fraction analysis for CPC-20 LP	35
8.	Sieve fraction analysis for Argonne samples E-11576 and E-11624	36
9.	Sieve fraction analysis for Argonne samples LST-1 and LST-4	37
10.	Sieve fraction analysis for Argonne samples CCS-10 and RGL-10	38
11.	Sieve fraction analysis for Exxon samples 30.1 and 32.0	39
12.	Sieve fraction analysis for Exxon samples 30.2 and 19.3	40

TABLES

Table		Page
I.	Chemical analysis of fluidized bed residues	15
II.	Chemical analysis of fluidized bed combustion-regeneration residues .	16
III.	Qualitative composition of fluidized bed residues from x-ray data . .	17
IV.	Test strengths of cured FBCR-sludge mixtures	22
V.	Conversion table of USA Standard Sieve Sizes	23

Section 1

INTRODUCTION

Residue materials produced by fluidized combustion of coal have been previously characterized in the published literature, but as a general rule such characterizations have been either limited to one sample source or have been reported as a minor part of some larger study.

It has been the primary purpose of this study to provide a comprehensive petrographic, mineralographic, and chemical characterization of fluidized bed combustion materials from a number of sources, including high- and low-pressure combustion beds and regeneration systems. With an eye towards beneficiation and/or disposal of these materials, auxillary studies have considered the particle size distribution found in these samples and their chemical composition as a function of size fraction and have investigated their use as stabilizing additives for flue gas desulfurization sludges.

These studies, both qualitative and quantitative, have used comparative optical and electron microscopy, x-ray diffraction, infrared analyses, and electron microprobe analyses to provide a comprehensive study of the composition and morphology observed in these samples.

This report presents data collected on fluidized bed combustion materials provided by the Argonne National Laboratory, the Combustion Power Company, and the Exxon Research and Engineering Company over the period July 1, 1975, to June 30, 1977.

Section 2

CONCLUSIONS

Bed material and flyash from high- and low-pressure fluidized bed combustors have been characterized petrographically, chemically, and with the aid of scanning electron microscopy, the electron microprobe, and x-ray powder diffraction. Granular bed materials generally consist of three zones. The outermost zone consists of a surface layer, or veneer, and ranges in thickness from 2 to 25 microns. This zone consists primarily of $CaSO_4$. Metallic oxides are generally present; their content is seen to range from a light Fe_2O_3 staining to heavy encrustations of siliceous glass containing large amounts of Fe_2O_3 (hematite) and Fe_3O_4 (magnetite). The physical integrity of this surface reaction zone is observed to range from an integral part of the granule body characterized only by color and crystallite size differences, to an easily separable physical shell which, while relatively hard, is not well associated with the body of the granule. The secondary reaction zone underlies this surface veneer; its thickness may range from 60 to 150 microns or, in well sulfated samples, to the granule's core. It consists of $CaSO_4$ and soft-burned CaO for limestone beds; MgO is sometimes seen with dolomite beds. Granules which have been incompletely sulfated will have a third zone or core consisting primarily of original material (with the exception of $MgCO_3$ which has not been observed) and small amounts of CaO or MgO.

Samples of regenerated bed materials have also been characterized. Those samples studied have been exposed to 10 cycles of sulfation and regeneration and are easily characterized by their outer layer which, while not necessarily thicker than that shown by once-through granules, is much higher in iron and silicon compounds and exists as a vitreous, amorphous, siliceous glass containing large amounts of Fe_2O_3 and Fe_3O_4. This encrustation is presumed to form gradually upon successive stages of regeneration.

Particle size fraction analyses have been performed on all samples. It has been shown that the content of $CaSO_4$ and $Ca(OH)_2$ generally increases with decreasing size fraction and that $CaCO_3$ is more concentrated in the larger fractions. The $Ca(OH)_2$ content increase in the smaller fractions is attributed to conversion of the softer CaO which is attrition ground from broken or fractured larger granules. SiO_2 has not shown a predictable composition relationship to size fraction. A sample described as "ash" is shown to consist primarily of finely ground $CaSO_4$. The process of fines transport from a fluidized bed and collection by cyclone is as likely to collect $CaSO_4$ as it is to collect "ash" since the ash component is seen to be concentrated on the surface of intact granules. Fines within the bed are likely to consist of the softer components of CaO and $CaCO_3$. These components are less resistant to attrition grinding by bed turbulence and will be quickly sulfated due to their high surface area to volume ratio.

It has been shown that fluidized bed combustion residue may be used to stabilize the $CaSO_3 \cdot 1/2H_2O$ sludges produced by wet lime/limestone scrubbing systems and that the fixed materials are not subject to resliming on contact with water. Short-term physical strengths appear to be higher for sludges containing flyash than for ash-free sludges. Increased strengths of stabilized materials are attributed primarily to formation of massive crystalline gypsum.

Section 3

INSTRUMENTAL TECHNIQUES OF CHARACTERIZATION

Fluidized bed combustion materials from the Argonne National Laboratory, the Combustion Power Company, and the Exxon Research and Engineering Company have been characterized. A number of techniques have been employed in this study. Scanning electron microscopy, using a Cambridge S-4 SEM, and optical microscopy have provided comprehensive petrographic and mineralographic information on these samples. An energy-dispersive x-ray analyzer was used in connection with the SEM to provide electron microprobe qualitative information regarding chemical composition of the materials.

X-ray powder diffraction of bulk samples and of separated size fractions was used to determine qualitative verification of petrographic data (as was infrared analysis) and to provide relative estimates of composition versus size fraction.

Various physical test equipment was used to determine unconfined compression strengths of materials as an indication of the degree to which they had been stabilized.

Section 4

SOLIDS CHARACTERIZATION

Samples of fluidized bed materials, bed reject materials, and flyash were obtained from combustors operated by the Combustion Power Company, Inc., the Argonne National Laboratory, and the Exxon Research and Engineering Company. Detailed results of the characterization studies on these samples are given below. Chemical analytical results are shown in Tables II and IV.

Combustion Power Company

One sample each of fluid bed material and flyash was received from a 20-inch (diameter) by 24-inch (depth) low-pressure combustor operated by the Combustion Power Company. The samples were obtained after 1003 hours of operation at 899°C from a test run. High (3.11 percent) sulfur coal was the fuel, dolomite was the sulfur dioxide absorbent (ratio of 0.24 lb of dolomite to 1.0 lb of coal), and Burgess No. 10 clay pigment was used as a corrosion suppressant (comprising 0.4 percent of the total bed weight). The results of chemical analyses of these samples are included in Table I.

The bed material sample was received in the form of orange to brick-red irregular granules of 0.5 to 1.0 mm in diameter (Figure 1A). Petrographic investigation indicates that this material consists primarily of $CaSO_4$ (anhydrite) and metallic oxides, mostly CaO, pseudomorphic after the original dolomite structure. Microchemical tests show Mg to be fairly abundant, although no free-formed magnesium salt could be identified; x-ray diffraction analysis indicates the existence of MgO. Most of the granules appear as dense units upon which a 2 to 5 micron hardened, reddish shell of hematite has been deposited. While the shell material itself is very hard, it is fairly easily separated from the body of the granule; a small percentage of the granules, as received, had sections of their "shell" broken away, exposing the softer body of the granule. The contrast between the comparatively smooth hematite surface coating and the coarser, crystalline, underlying layer of $CaSO_4$ is readily seen in Figures 1B and 1C. Towards the center of the granules, the $CaSO_4$ occurs in a more massive form (Figure 1D); a high percentage of the anhydrite is optically amorphous. Qualitative analyses of the total granule material by x-ray powder diffraction verify $CaSO_4$ as the major phase, with lime (CaO) being present in somewhat lesser quantities. Quartz, $Ca(OH)_2$, and MgO are present in small amounts.

The flyash portion of this sample was received in the form of finely divided, 5- to 25-micron, orange-red solids (Figures 1E and 1F). The major fraction of this material is $CaSO_4$, part of which is crystalline.

Microchemical tests show that part of the $CaSO_4$ is present as soluble anhydrite; i.e., addition of water to the sample results in the formation of a significant quantity of gypsum. Hematite is observed petrographically as a minor phase with quartz, CaO, and a clay-like siliceous material all present in trace quantities. X-ray powder diffraction analyses indicates, in addition to the components mentioned above, the presence of $CaSO_4 \cdot 3MgSO_4$ in trace quantities.

Argonne National Laboratory

Sample E-11576 was taken from a high-pressure fluidized bed combustor, 6 inches in width and with a bed depth of 3 feet, operated at 900°C at a pressure of 8 atmospheres. The fluidizing gas velocity (with 17 percent excess air) was approximately 0.9 m/s and Grove limestone was used as the absorbent at a Ca:S molar feed ratio of 1:5. The sample was received in the form of dark brown granules with diameters ranging from 0.1 to 1.5 mm. Petrographic examination indicates that the granules consist primarily of $CaSO_4$ and $CaCO_3$, with small amounts of CaO. Microchemical tests indicate trace quantities of soluble anhydrite. Qualitative analyses by x-ray diffraction and infrared spectrophotometry verify the presence of anhydrite, limestone, and lime, including trace amounts of quartz and hematite. A given individual granule will be covered with an outer layer up to 25 microns in thickness consisting of $CaSO_4$ and Fe_2O_3. The thickness of this outer veneer will determine the color of the granule, with the lighter colored granules having thinner veneers. Under this surface coating another zone is observed, ranging up to 100 microns and consisting of $CaSO_4$ and soft-burned, amorphous CaO. These granules show a core or central zone of poorly crystallized $CaCO_3$ and CaO, ranging in diameter from 500 to 900 microns.

A second sample (E-11624) was taken from the combustion system described above with the stated operating conditions, but using Tymochtee dolomite as the absorbent. The sample was received in the form of light brown granules, with diameters ranging from 0.1 to 1.5 mm. Petrographic examination shows that the granules consist chiefly of aggregates of $CaSO_4$ and soft-burned, amorphous MgO and contain approximately 10 to 20 percent $CaCO_3$. In this sample, the outer layer is only 5 microns in thickness (accounting for the lighter color) and consists of anhydrite, Fe_2O_3, and dead-burned MgO. The second zone in this sample extends to the core of the particle and consists of $CaSO_4$ and soft-burned MgO (possibly a form of $MgO-MgCO_3-Mg(OH)_2$ solid solution) which is amorphous with a refractive index of approximately 1.64. The presence of anhydrite, $CaCO_3$, and MgO is verified by x-ray diffraction. Semiquantitative infrared spectrophotometric analyses show a gross sample composition of approximately 80 percent sulfate and 20 percent carbonate, with small amounts of CaO, Fe_2O_3, and quartz.

Four additional samples were obtained from the Argonne National Laboratory. The samples consisted of both spent (sulfated) and regenerated granular materials from limestone and dolomite beds. Samples LST-1 (originally Columbia limestone) and LST-4 (originally Georgia marble) were removed from a fluidized combustion system operated at 870°C and approximately 4 atmospheres. The Ca:S ratios used in the two tests were 1.6 and 2.2, respectively. The fluidizing gas velocity (containing 17 percent excess air) was 0.76 m/s for LST-1 and 0.82 m/s for LST-4. Samples CCS-10 (originally Tymochtee dolomite) and RGL-10 (originally Greer limestone) were obtained from fluidized bed combustion-regeneration systems operated at 1100°C and approximately 1.5 atmospheres after 10 cycles of regeneration. The gas velocity used was 1.2 m/s.

In sample LST-1, petrographic examination indicates that three major types of particles are present. Approximately 10 percent of these consist of $CaCO_3$ as single rhombic crystals up to 1200 microns in length, with a thin (up to 20 microns) surface veneer of reaction product which is present as single-plate crystals of $CaSO_4$ up to 10 microns across. Another 15 percent of the sample occurs as anhydrite crystals aggregated into units with a maximum size of 150 microns. The individual $CaSO_4$ crystals comprising these aggregates may range up to 15 microns and are very slowly soluble in hot, concentrated acids. The other three-fourths of the sample is coarse granular aggregates of $CaCO_3$ with a 25-micron surface veneer of $CaSO_4$ as plate crystals with a maximum length of 15 microns. This veneer shows iron staining with iron present as Fe_2O_3. The presence of numerous agglomerated fines shows that the sample has been subjected to a long period of attrition grinding.

Sample LST-4 is similar in color and appearance to LST-1; about two-thirds of the sample occurs as granular aggregates up to 1200 microns in diameter. These granules consist of $CaCO_3$ crystals with a 35-micron surface veneer. This outer layer is formed of $CaSO_4$ crystals with a maximum dimension of 15 microns and shows a small amount of iron staining as Fe_2O_3. Approximately one-fourth of the sample is single crystals of $CaCO_3$ up to 1200 microns across and coated with a 15-micron surface layer of $CaSO_4$. Less than 10 percent of the sample material occurs as 250-micron $CaCO_3$ aggregates stained with Fe_2O_3. Virtually all of the $CaSO_4$ present in this sample is the insoluble anhydrite form.

Neither of the two samples, LST-1 or LST-4, exhibits discrete, defined, reaction zones (except for external layer formation) as do the previously examined sulfated materials. Granules of both of these samples were prepared for SEM examination by embedding them in an epoxy potting compound and grinding the resultant solid to reveal a cross section of their internal structures. Optical photomicrographs of the samples thus prepared are shown in Figures 2A and 2B. The mottled appearance of most granules and lack of obvious zone formation support the assumption that, depending on the particle porosity, sulfation and contamination by inerts proceeds within the particle at a slower rate than on the surface. The lack of reaction zone formation is attributed

to this difference in porosity; less densely aggregated stones are more likely to show such formations.

Patterns of interior sulfation along grain boundaries are easily seen when the prepared granules are lightly etched with hydrochloric acid. This procedure dissolves away the highly soluble $CaCO_3$ component, while leaving the $CaSO_4$ portion relatively untouched. Figure 3A shows a SEM photomicrograph of such an etched particle. The web-like nature of the $CaSO_4$ is easily seen, sulfation having proceeded along internal surface areas provided by the granule's porosity. The relatively smoother area seen on all sides but the lower left of the web structure is the unetched surface of the potting compound. Figures 3B and 3C show views of a cross section of another granule, both before and after etching. The internal network of $CaSO_4$, barely visible as trace outlines on the unetched granule (Figure 3B), is clearly seen after etching (Figure 3C). The relatively darker or smoother region in the lower right corner of the photograph is again unetched potting compound.

Figures 3D and 3E show an example of edge (surface) sulfation on a granule of sample LST-4. In Figure 3D, the thin surface of sulfation (seen in cross section) is only faintly visible. After light etching (Figure 3E) this layer clearly stands out. Electron microprobe analysis verifies that sulfur is a major component of this edge structure and is present only in residual amounts in the body of the particle. The deep longitudinal dissolution features running northeast to southwest on the photograph are artifacts resulting from preferential dissolution of the $CaCO_3$ along lattice planes caused by localized lattice defects of a nonstoichiometric nature, or strain effects caused by grinding.

Samples CCS-10 and RGL-10 were received in the form of 0.5 to 1.0 mm dark brown to black granules, with less than 5 percent of the material present as fines of less than 60 mesh (see Table V for conversion to microns).

Upon petrographic examination, two basic types of particles are seen in sample RGL-10. One-fourth of the sample consists of black, magnetic units consisting of a siliceous glass (refractive index of 1.545) and black opaque particles of magnetite present as cubic pseudomorphs--possibly after pyrite. These particles produce a sulfide odor upon dissolution in HCl. Approximately two-thirds of the sample is present as brown, iron oxide-stained granules of CaO with a 10- to 12-micron surface veneer consisting of a mixture of $CaSO_4$ (about 1 micron crystals), siliceous glass, and an occasional black, magnetic, cubic pseudomorph at the surface. The CaO approaches a dead-burned condition; it has a mean refractive index of 1.77 to 1.78. The iron content of this sample appears to be unusually high. This may be a result of a gradual buildup of metallic oxides during successive cycles of combustion and regeneration. The occurrence of soluble anhydrite in this sample is negligible.

Sample CCS-10 consists of two types of particles. About 15 percent are magnetic and consist of a deeply colored glass having a mean refractive index of 1.70 to 1.74, with a trace of incipient crystallization of unknown composition (possibly an iron silicate). Cubic pseudomorphs are a significant component of this magnetic fraction. The remainder of the granules range from light brown to dark gray in color due to various degrees of iron staining in the outer 10-micron veneer. This surface layer consists of an amorphous slag and overlies a secondary reaction zone, approximately 40 microns in thickness, consisting of $CaSO_4$. The core of these granules is composed of $CaCO_3$ and MgO. The core MgO component is soft-burned. No soluble anhydrite was found in this sample.

Both RGL-10 and CCS-10 were prepared for SEM examination by the embedding and grinding process described previously. Figures 4A and 4B show optical photomicrographs of the prepared samples; note examples of surface encrustations of metallic oxides and reaction zones exposed in the cross-sectional views of several granules (marked by arrows).

Figures 5A and 5B show cross-sectional views of representative CCS and RGL granules. The thick vitreous crust of inert material which interferes with both regeneration and sulfation is easily seen; it is shown by electron microprobe analysis to contain a high percentage of aluminum, silicon, and iron. Similar analyses of the granules' interior regions show a preponderance of calcium, or where dolomite is used, calcium and magnesium.

The decreased reactivity of absorbent after successive cycles of regeneration is attributed primarily to crust formation. No evidence of sintering in the core of these granules has been observed.

Exxon Research and Engineering Company

Sample 19.3 (bed materials) was removed from a high-pressure combustor operated at a temperature of 900°C and a pressure of 9 atmospheres for a period of 6 hours. The bed dimensions were 12.5 inches wide by 4.7 feet deep; the gas velocity (at 6 percent excess air) was 1.9 m/s. Grove limestone was used as the absorbent with a molar feed ratio Ca:S of 1.5. Received in the form of dark brown granules averaging 1 mm in diameter, a quantity of fines was also observed, presumably as the result of fracture of the larger granules (which are not structurally strong) by circulation within the bed or in handling or shipping. Petrographic examination shows that the granules have a surface layer up to 5 microns thick of $CaSO_4$ and Fe_2O_3. The remainder of the granule is generally divided equally between a secondary reaction zone containing $CaSO_4$ and CaO and a central core section composed of $CaCO_3$ and CaO. X-ray powder diffraction and infrared analyses identify $CaSO_4$ and $CaCO_3$ as major components present in a 2:3 ratio with CaO, Fe_2O_3, and quartz all present in amounts smaller than 5 percent.

Sample 30.1 (bed reject materials) was removed from the combustor as described for the previous sample with the same operating conditions except that a Ca:S molar feed ratio of 3.7 was used, and the amount of excess air was increased to 13.7 percent. As received, the sample consisted of dark brown granules ranging in diameter from 1 to 2 mm. Optical microscopic examination reveals that these granules also consist of three separate and distinct zones. The surface of the granules is covered with a thin (up to 5 microns) layer of dead-burned CaO, insoluble anhydrite, and Fe_2O_3. Underneath this layer, ranging in thickness from 60 to 150 microns, lies a second zone of soluble anhydrite and soft-burned CaO. The central zone, or core, consists chiefly of poorly crystalline $CaCO_3$ and soft-burned CaO. X-ray diffraction studies of the bulk sample verify the presence of these components and show, in addition, small quantities of quartz. Semiquantitative infrared analyses indicate a $CaCO_3$ to $CaSO_4$ ratio of 3:1, and identify CaO, quartz, and Fe_2O_3 present in amounts smaller than 5 percent total.

Sample 30.2 (bed reject materials) was obtained from the combustor as described above. During this run, a Ca:S ratio of 3.7 was used, the bed temperature was raised to 930°C, and 17% excess air was used as the fluidizing gas at a velocity of 8 feet/sec. This sample consisted of brown to black granules ranging in diameter from 0.5 to 2.5 mm. While easily crushed with fingertip pressure, these granules are much stronger structurally than previous Exxon samples. Here, the outer layer is 3 to 5 microns thick and again consists of $CaSO_4$ and metallic oxides, but the second reaction zone composes the bulk of the particle; little or no core zone exists. Qualitative analysis by x-ray indicates primarily $CaSO_4$ and CaO; but infrared studies show, in addition, smaller quantities of $CaCO_3$, Fe_2O_3, and quartz. A $CaCO_3$ to $CaSO_4$ ratio of 1:12 is indicated.

Sample 32.0 consisted of bed materials removed from a run in which Pfizzer dolomite was used as the absorbent. This test run was made at a pressure of 5.9 atmospheres and at 840°C; 20 percent excess air was used at a velocity of 1.5 m/s. A Ca:S ratio of 0.75 was used. The sample was received in this laboratory in the form of dark brown to black granules with approximate sizes ranging from 0.5 to 2 mm. The surface veneer in these particles is between 3 to 10 microns in thickness, consisting of $CaSO_4$, Fe_2O_3, and hard-burned MgO (collapsed, dense, crystalline units with a refractive index of 1.735). The secondary zone of reaction constitutes the major fraction of the granule and is composed of $CaCO_3$ and soft-burned, amorphous MgO. The small center zone consists of poorly crystalline $CaCO_3$ and soft-burned MgO. Infrared analysis of the rock sample shows the presence of $CaCO_3$ and $CaSO_4$ with a 1:5 ratio. Traces of CaO, quartz, and Fe_2O_3 are also indicated. MgO is shown by x-ray diffraction studies.

Samples of the above materials were mounted and subjected to grinding and polishing as previously described to expose cross sections of the granules for observation. Figures 6A, 6C, and 6E show SEM photomicrographs of granule sections as viewed with secondary electron imaging

(normal SEM operating mode). The secondary reaction zone in these granules is seen as that area near the periphery of each granule which is relatively smoother than the granule interior. This relatively smooth appearance is due to the fact that this $CaSO_4$-containing zone is generally harder than the $CaCO_3$-CaO core zone and thus more resistant to abrasion. In these sections the secondary zone extends from 50 to 200 microns into the body of the granule. The irregular white tracing superimposed on Figure 6A indicates the sulfur content of the section immediately below the line. As this tracing approaches the left edge of the granule it rises sharply, indicating an increase in sulfur content at the particle's periphery, then drops back to a low level across the granule's interior region indicating that sulfation has not yet proceeded to completion. The sulfur content again rises as the electron beam reaches the right edge of the granule.

Figures 6B, 6D, and 6F correspond to the views shown on the left-hand side of the page but show the granules' cross section as viewed by the 2.307 kev (sulfur) x-rays as emitted by the sample when struck by the scanning electron beam. These photographs may be described as "sulfur maps" of the granules and show the relative distribution of sulfur on and within the granule. The usually peripheral secondary reaction zone is shown to be rich in sulfur, but note Figure 6F where sulfation has proceeded along structural cracks into the body of the granule.

Section 5

SIZE CLASSIFICATION AND X-RAY STUDIES

Samples (as received) of fluidized bed materials were subjected to size classification by dry seiving and x-ray powder diffraction analysis to determine the general composition of various size fractions and the compositional differences between them. The seive analyses are reported in Figures 7 through 12, and the fraction composition data are shown in Table III.

The samples of bed materials and flyash from the Combustion Power Company show the expected size distributions. Two-thirds of the bed materials are +100 mesh while two-thirds of the flyash (collected from a second-stage cyclone) is sized below 200 mesh. For mesh size-micron conversion, see Table V. In the bed material the content of $Ca(OH)_2$ is seen to increase with decreasing particle size. Since the largest fractions are whole granules with a relatively intact inert outer shell, only the smaller, broken granules will expose unreacted CaO to the atmosphere, forming the $Ca(OH)_2$. The bulk of the ash material (-200 mesh) is seen to consist of the same material as reported by petrographic analysis ($CaSO_4$, SiO_2, and Fe_2O_3).

The two high-pressure (8 atmospheres) bed samples from the Argonne National Laboratory (E-11576 and E-11624) are interesting in that they display such differences in particle size distribution. The sample containing the largest (more than 30 percent) amount of -60 mesh particles is E-11576. This sample has a 25-micron outer layer, whereas E-11624 (derived from dolomite) has only a 5-micron shell. Since this outer, relatively inert, layer is usually structurally stronger than the core of the granule, one would expect, under similar conditions, more attrition grinding to be evidenced by the sample with the thinner shell. While the sample E-11576 may have been subjected to more turbulent conditions within the bed or rougher handling before receipt by this laboratory, another possibility is that the inert shell on this sample, while quite strong itself, is not particularly well cemented to the particle body. The outer veneer on some samples has been observed to be weakly "attached" to the granule body; in some cases it may easily be flaked off. This would have exposed the much softer granule interior to further fracture and attrition grinding during any subsequent handling step. In sample E-11576, the content of CaO is seen to decrease with decreasing particle size. Furthermore, there is an accompanying increase in $Ca(OH)_2$ content as the exposed lime is hydrated.

Samples LST-1 and LST-4, from 4 atmosphere beds, show essentially the same particle size distribution with three-fourths of each sample being larger than 60 mesh. In both samples, the content of both CaO and $Ca(OH)_2$ are seen to increase with decreasing size fraction, the increase

in $Ca(OH)_2$ being dependent on exposure of CaO. SiO_2 is a relatively constant component of LST-4. It is useful to consider that the stone used for LST-4 contained 1.3 weight percent of SiO_2 initially, as compared to 0.2 percent for the limestone that produced LST-1. For both samples, the $CaSO_4$ content increases with the smaller fractions and the $CaCO_3$ content decreases.

Again, samples CCS-10 and RGL-10 (10th cycle of regeneration) show the same particle size distribution. The dolomite-derived material (CCS-10) shows major amounts of MgO throughout all size ranges although its $CaSO_4$ component is still present in noticeable quantities, indicating regeneration has not been completely successful. In both samples, $Ca(OH)_2$ increases with decreasing particle size, as more residual or regenerated CaO is exposed to the atmosphere. Both the Fe_3O_4 and $MgO \cdot 2CaO \cdot 2SiO_2$, which are found in trace amounts throughout all size ranges, are assumed to originate on the surface veneer of the granules during the combustion cycle.

Exxon sample 30.1 contains about 30 weight percent minus 60-mesh material. Over the size range of solids shown, both the $CaSO_4$ and CaO content increase with decreasing particle size. Exxon sample 32 (dolomite bed) shows the same general size distribution, but here the $CaSO_4$ content is roughly constant. In both samples, $CaCO_3$ generally decreases with decreasing particle size. In Exxon 30.2, both CaO and $CaSO_4$ are fairly constant regardless of size fraction. This sample contains less than 3 weight percent minus 60-mesh material, indicating very little attrition grinding has taken place. Again, the $Ca(OH)_2$ component increases with decreasing particle size.

In summary, within the range of samples studied the content of both $CaSO_4$ and $Ca(OH)_2$ is seen generally to increase with decreasing particle size, while $CaCO_3$ content decreases under the same conditions.

Section 6

FLUIDIZED BED MATERIAL--SLUDGE STABILIZATION TESTS

Sludges produced by wet lime/limestone SO_2 scrubbing systems have produced severe disposal problems. A partial solution to this problem lies in fixing or stabilizing this sludge with various additives. Several commercial processes exist to accomplish this. It has been suggested that fluidized bed combustion residues may also be used to stabilize these sludges. In an attempt to determine the feasibility of this idea and to develop a simple laboratory stabilization test procedure, fixation tests were performed with fluidized bed combustion residue and sludges produced from two different wet scrubbing systems.

The fluidized bed material used was a 1:1 ratio of the Combustion Power Company bed material and second-stage flyash. The bed material was ground to -200 mesh before mixing. On a weight percent basis, sludge number 1 consisted of approximately 30 percent ash, 8 percent $CaSO_4 \cdot 2H_2O$, 54 percent $CaSO_3 \cdot 0.5H_2O$, and 8 percent $CaCO_3$. Sludge number 2 contained about 1 percent ash, 9 percent $CaSO_4 \cdot 2H_2O$, 77 percent $CaSO_3 \cdot 0.5H_2O$, and 14 percent $CaCO_3$. The solids component of both sludges was essentially -200 mesh.

The sludges used were allowed to drain on a filter to remove most of the liquor, which was saved. Appropriate amounts of fluidized bed material and sludge were then mixed with sufficient amounts of liquor added to achieve approximately 75 weight percent solids. Cylindrical cores of the resulting mixture measuring 4 cm in length and 2 cm in diameter were separated and allowed to cure in a container held at room temperature and 100 percent humidity from 5 to 11 days. The unconfined compression strength of the cured pellets was then measured.

The results of these tests are shown in Table IV. The compressive strength increases with time and is directly related to the percent of fluidized bed residue in the original mixture. Pellets produced from sludge number 2, containing essentially no flyash, were noticeably weaker. For all mixtures, pellet fragments immersed in boiling water for 1 day exhibited no resliming.

X-ray diffraction examination of the fixed pellets indicated that a large quantity of gypsum ($CaSO_4 \cdot 2H_2O$) has been formed, presumably by hydration of the soluble anhydrite component in the fluidized bed material. SEM examination indicates large, massive gypsum crystal growth throughout the body of the sample. This type of structure has been seen in gypsum scale removed from the internal surfaces of wet limestone SO_2 scrubbing towers. The strength of this material is primarily attributed to this massive and interlocking internal crystal growth.

TABLE I

Chemical Analysis (Weight Percent)

Constituent	CPC 20" LP bed	CPC 20" LP ash	Exxon Run 19.3	Exxon Run 30.1	Exxon Run 30.2	Exxon Run 32.0	Argonne Run E-11624	Argonne Run E-11576
Na^{+}	0.07	0.14	0.01	ND[a]	ND[a]	ND[a]	0.05	ND[a]
K^{+}	0.04	0.13	0.03	0.02	0.02	0.01	0.14	ND[a]
Cl^{-}	ND[a]	<0.1	<0.1	ND[a]	ND[a]	ND[a]	ND[a]	ND[a]
Ca^{+2}	23.0	12.7	35.9	36.0	47.0	34.8	22.7	35.9
Mg^{+2}	13.1	6.4	0.36	2.6	1.1	6.0	14.0	0.39
CO_2^{-2}	0.4	1.3	33.5	36.0	2.6	11.9	7.6	20.5
SO_3^{-2}	ND[a]	<0.1	0.1	ND[a]	ND[a]	ND[a]	ND[a]	ND[a]
SO_4^{-2}	29.7	33.6	14.7	14.2	25.9	29.5	34.7	31.2
Si	11.1	0.55	0.44	0.29	0.62	0.40	0.96	0.47
Fe	1.7	0.95	0.72	0.39	0.68	0.67	0.36	0.48
Al	0.72	0.51	0.26	0.15	0.34	0.21	0.50	0.31
Acid insolubles	14.7	36.0	4.3	2.1	2.8	3.7	3.7	1.8

[a]ND = not determined.

TABLE II

Chemical Analysis (Weight Percent)[a]

Constituent	CCS-10	RGL-10	LST-1	LST-4
S	3.2	1.0	8.0	6.3
$CO_3^=$			35.6	36.8
Ca	25.7	37.6	36.5	33.6
Mg			1.0	
C			8.2	7.1
Si	6.1	10.4	0.9	
Al_2O_3			2.2	
Fe_2O_3			0.6	

[a]Analytical data supplied by Argonne National Laboratory.

TABLE III

Qualitative Composition From X-Ray Data[a]

Sample	$CaSO_4$	CaO	$CaCO_3$	$Ca(OH)_2$	SiO_2	MgO	Fe_2O_3	Other
				CPC 20" LP bed material				
+30	m	-	-	-	M	-	tr	
-30 to +60	M	tr	-	tr	m	m	-	
-60 to +100	M	tr	tr	m	-	m	-	
-100 to +200	M	-	-	m	tr	m	-	
-200 to +400	M	-	tr	tr	tr	m	-	
-400	M	tr	tr	m	tr	m	-	
				CPC 20" LP ash				
+30	M	-	-	-	m	tr	m	$CaSO_4 \cdot 3MgSO_4$ (M)
-30 to +60	M	-	-	-	m	tr	m	$CaSO_4 \cdot 3MgSO_4$ (m)
-60 to +100	M	-	-	-	m	tr	tr	$CaSO_4 \cdot 3MgSO_4$ (m)
-100 to +200	M	-	-	-	m	tr	m	$CaSO_4 \cdot 3MgSO_4$ (m)
-200 to +400	M	-	-	-	m	-	m	$CaSO_4 \cdot 3MgSO_4$ (m)
-400	M	-	-	-	M	-	m	$CaSO_4 \cdot 3MgSO_4$ (m)
				Argonne E-11576				
+20	M	m	M	-	tr	-	-	
-20 to +30	M	m	M	-	tr	-	-	
-30 to +60	M	m	M	-	tr	-	-	
-60 to +100	M	tr	m	tr	-	-	tr	
-100 to +200	M	tr	m	tr	-	-	-	
-200	M	tr	m	m	-	-	-	

[a] M > 30% (major); 30% > m > 5% (minor); tr < 5% (trace).

TABLE III (continued)

Qualitative Composition From X-ray Data[a]

Sample	$CaSO_4$	CaO	$CaCO_3$	$Ca(OH)_2$	SiO_2	MgO	Fe_2O_3	Other
				Argonne E-11624				
+20	M	-	m	-	tr	m	-	$CaMg(CO_3)_2$ (tr)
-20 to +30	M	-	m	-	tr	m	-	
-30 to +60	M	-	tr	-	m	m	-	$CaMg(CO_3)_2$ (tr)
-60	M	tr	m	tr	tr	m	-	$CaMg(CO_3)_2$ (tr)
				Argonne LST-1				
+20	m	-	M	-	-	-	-	
-20 to +30	m	-	M	-	-	-	-	
-30 to +60	m	tr	M	-	-	-	-	
-60 to +100	M	m	m	tr	-	-	-	
-100 to +200	M	tr	m	tr	-	-	-	
-200	M	tr	m	m	-	-	-	
				Argonne LST-4				
+20	m	-	M	-	tr	-	-	
-20 to +30	m	-	M	-	tr	-	-	
-30 to +60	m	-	M	-	tr	-	-	
-60 to +100	M	tr	M	-	tr	-	-	
-100 to +200	M	tr	M	tr	tr	-	-	
-200	M	tr	m	tr	-	-	-	

[a] M > 30% (major); 30% > m > 5% (minor); tr < 5% (trace).

TABLE III (continued)

Qualitative Composition From X-ray Data[a]

Sample	$CaSO_4$	CaO	$CaCO_3$	$Ca(OH)_2$	SiO_2	MgO	Fe_2O_3	Other
				Argonne CCS-10				
+20	m	m	-	tr	tr	M	tr	
-20 to +30	m	tr	-	tr	tr	M	m	
-30 to +60	m	m	-	tr	tr	M	m	
-60	m	m	-	m	tr	M	tr	
				Argonne RGL-10				
+20	m	M	-	tr	M	tr	m	Fe_3O_4 (tr), $MgO \cdot 2CaO \cdot 2SiO_2$ (tr)
-20 to +30	tr	M	-	tr	m	tr	tr	Fe_3O_4 (tr), $MgO \cdot 2CaO \cdot 2SiO_2$ (tr)
-30 to +60	tr	M	-	m	m	tr	tr	Fe_3O_4 (tr), $MgO \cdot 2CaO \cdot 2SiO_2$ (tr)
-60	m	M	-	M	M	tr	m	Fe_3O_4 (tr), $MgO \cdot 2CaO \cdot 2SiO_2$ (tr)
				Exxon 30.1				
+12	m	-	M	-	tr	tr	-	
-12 to +20	m	-	M	-	tr	tr	-	
-20 to +30	m	-	M	tr	tr	tr	tr	
-30 to +60	M	tr	M	-	tr	tr	tr	Fe_3O_4 (tr)
-60 to +100	M	tr	m	-	-	tr	tr	
-100 to +200	M	tr	m	tr	-	tr	tr	
-200 to +400	M	tr	m	m	tr	tr	-	
-400	M	tr	M	m	-	-	-	

[a] M > 30% (major); 30% > m > 5% (minor); tr < 5% (trace).

TABLE III (continued)

Qualitative Composition From X-ray Data[a]

Sample	$CaSO_4$	CaO	$CaCO_3$	$Ca(OH)_2$	SiO_2	MgO	Fe_2O_3
			Exxon 32				
+12	M	tr	m	-	tr	m	-
-12 to +20	M	m	m	-	tr	m	-
-20 to +30	M	M	m	-	tr	tr	-
-30 to +60	M	M	m	tr	-	tr	-
-60 to +100	M	M	tr	tr	-	tr	-
-100 to +200	M	m	tr	tr	-	tr	-
-200 to +400	M	m	tr	m	-	-	tr
-400	M	m	tr	m	-	-	-
			Exxon 30.2				
+12	M	M	tr	tr	tr	-	-
-12 to +20	M	M	-	tr	tr	-	-
-20 to +30	M	M	-	tr	tr	-	tr
-30 to +60	M	M	-	m	tr	-	m
-60 to +100	M	M	tr	m	-	-	-
-100	M	M	tr	M	tr	-	-

[a] M > 30% (major); 30% > m > 5% (minor); tr < 5% (trace).

TABLE III (concluded)

Qualitative Composition From X-ray Data[a]

Sample	$CaSO_4$	CaO	$CaCO_3$	$Ca(OH)_2$	SiO_2	MgO	Fe_2O_3
			Exxon 19.3				
+12	M	-	m	-	tr	-	-
-12 to +20	M	tr	m	-	tr	-	-
-20 to +30	M	-	m	-	tr	-	-
-30 to +60	M	tr	m	-	tr	-	-
-60 to +100	M	m	tr	tr	-	-	tr
-100 to +200	M	m	tr	tr	-	-	-
-200 to +400	M	m	tr	m	-	-	tr
-400	M	m	tr	m	-	-	-

[a] M > 30% (major); 30% > m > 5% (minor); tr < 5% (trace).

TABLE IV

Test Strengths of Cured FBCR-Sludge Mixtures

Test Number	Composition on solids basis (weight percent)			Unconfined compression strength (cured at room temp. and 100% humidity)		
	FBC	Sludge 1	Sludge 2	5 days	8 days	11 days
1	100	0	0	300	480	NT[a]
2	90	10	0	280	350	400
3	75	25	0	220	270	300
4	50	50	0	70	90	120
5	25	75	0	60	80	100
6	90	0	10	240	250	250
7	75	0	25	200	220	200
8	50	0	50	100	110	140
9	25	0	75	50	50	70

[a]NT = not tested.

TABLE V

Conversion Table of USA Standard Sieve Sizes

USA standard	Microns
12	1700
20	850
30	600
60	250
100	150
200	75
400	38

Figure 1

Scanning electron micrographs for Combustion Power Corporation sample 20 LP.

A. 200-diameter view of bed material granules
B. 1000-diameter view of broken surfaces of granule showing crystalline interior
C. 2000-diameter cross-sectional view of granule surface showing surface layer and crystalline interior
D. 2000-diameter view of crystalline interior of granule
E. 200-diameter view of second stage "ash" particles
F. 1000-diameter view of second stage "ash" granules

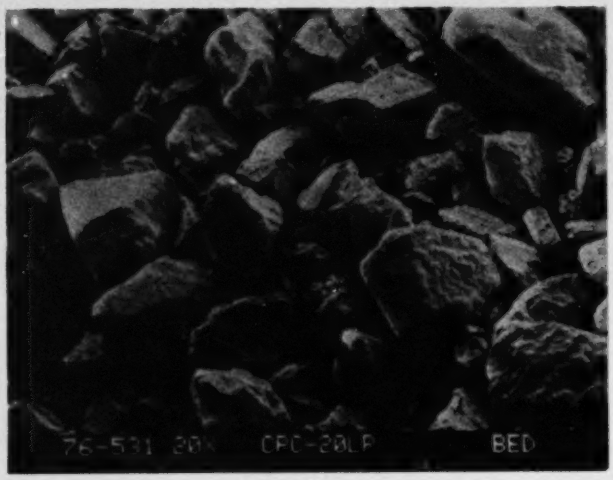

Figure 1A

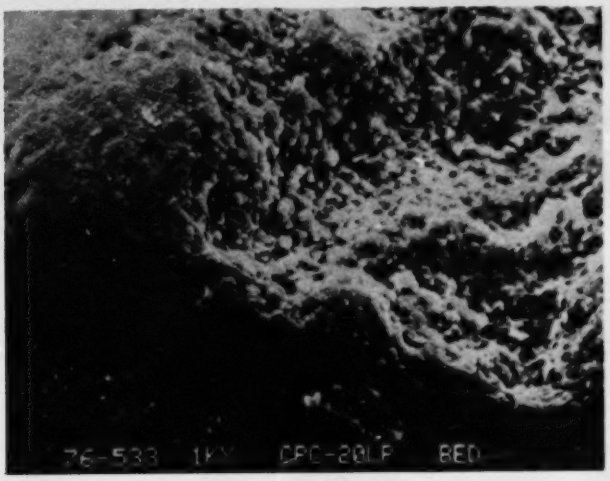

Figure 1B

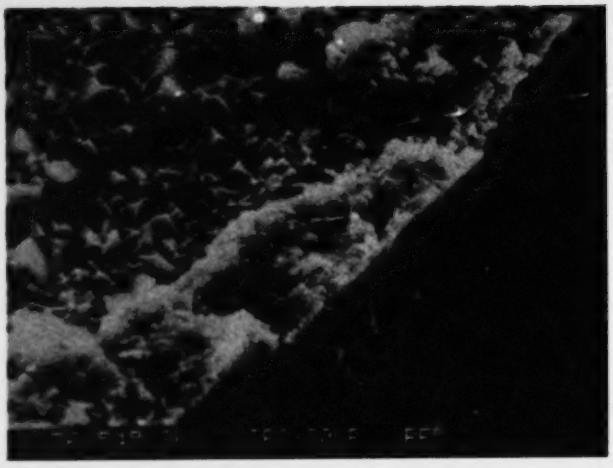

Figure 1C

Figure 1D

Figure 1E

Figure 1F

Figure 2

Optical photomicrographs for Argonne samples LST-1 and LST-4.

A. 16-diameter view of polished cross sections of LST-1 granules
B. 16-diameter view of polished cross sections of LST-4 granules

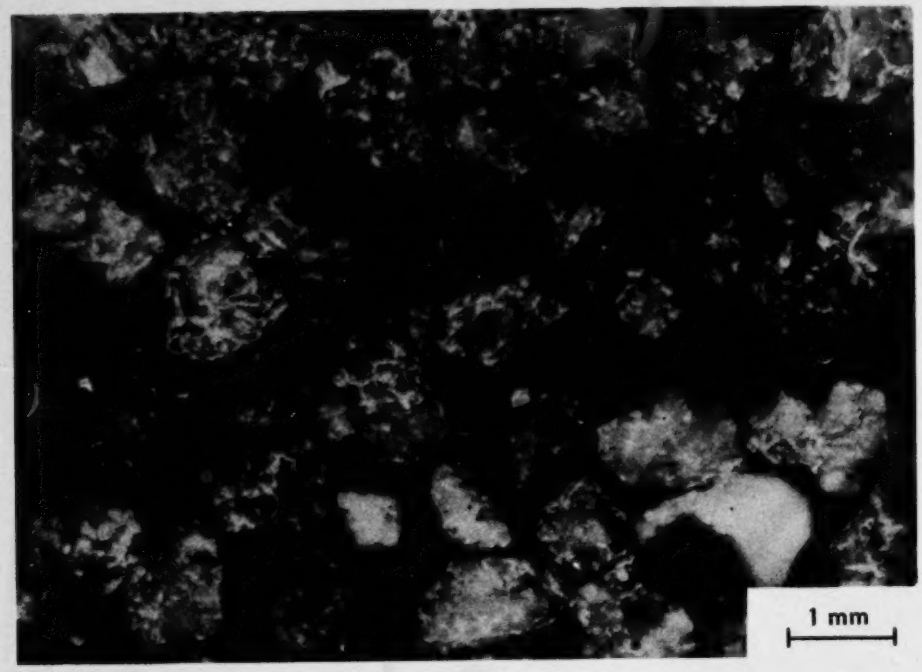

LST-1
Figure 2A

LST-4
Figure 2B

Figure 3

Scanning electron micrographs for Argonne samples LST-1 and LST-4.

A. 100-diameter view of etched cross section of LST-1 bed granule
B. 200-diameter view of polished cross section of LST-1 granule
C. 200-diameter view of etched cross section shown in (B)
D. 500-diameter view of polished cross section of granule showing edge of granule
E. 500-diameter view of etched section shown in (D)

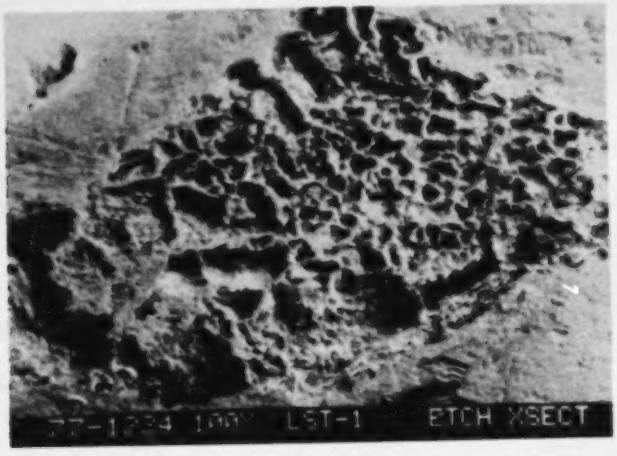

Figure 3A

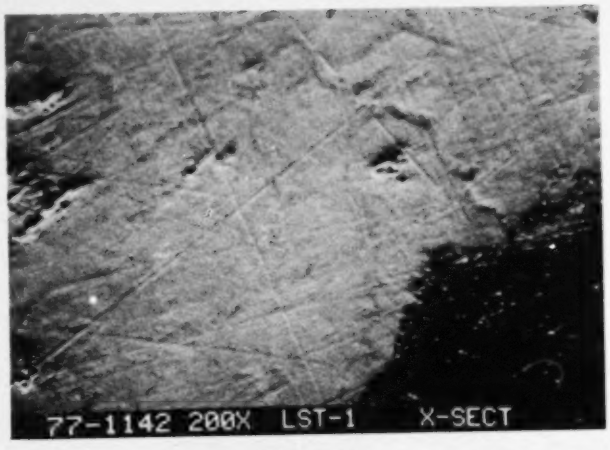

Figure 3B

Figure 3C

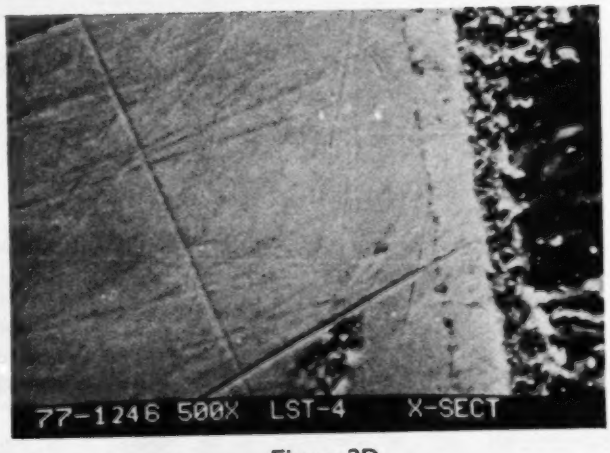

Figure 3D

Figure 3E

Figure 4

Optical photomicrographs for Argonne samples CCS-10 and RGL-10.

A. 16-diameter view of polished cross sections of sample CCS-10 granules. Arrows explained in text show edge layering and reaction zone features.
B. 16-diameter view of polished cross sections of sample RGL-10 granules. Arrows explained in text show edge layering and reaction zone features.

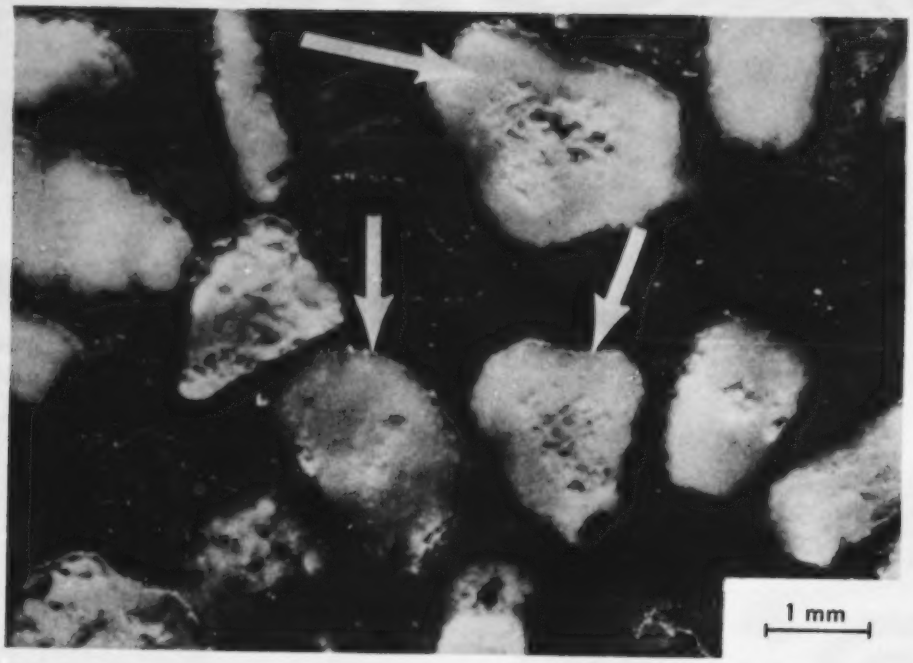

CCS-10
Figure 4A

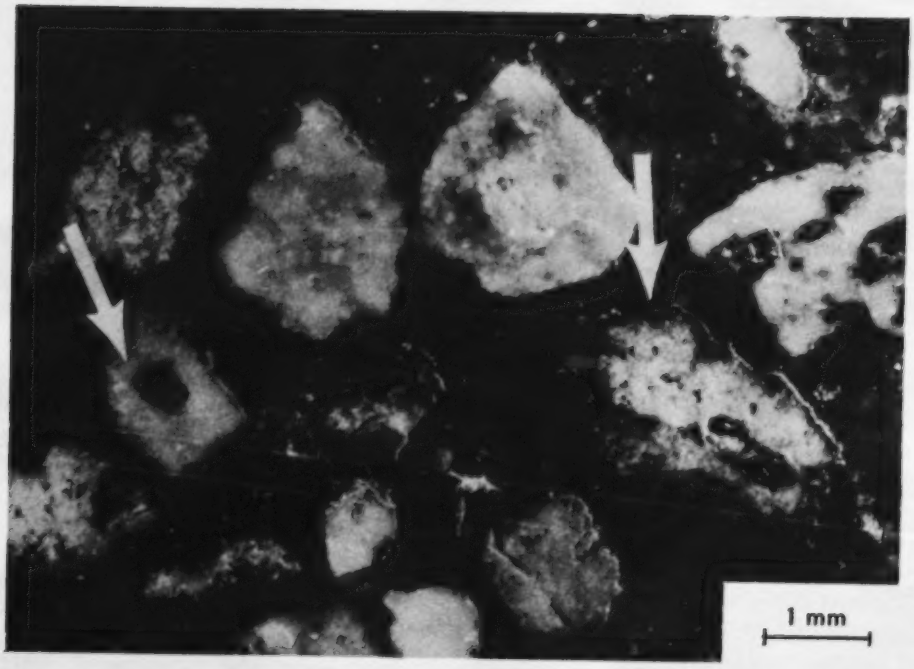

RGL-10
Figure 4B

Figure 5

Scanning electron micrographs for Argonne samples CCS-10 and RGL-10.

A. 50-diameter view of etched cross sections of CCS-10 granules; electron probe elemental analysis shown for indicated areas
B. 50-diameter view of etched cross sections of RGL-10 granules; electron probe elemental analysis shown for indicated areas

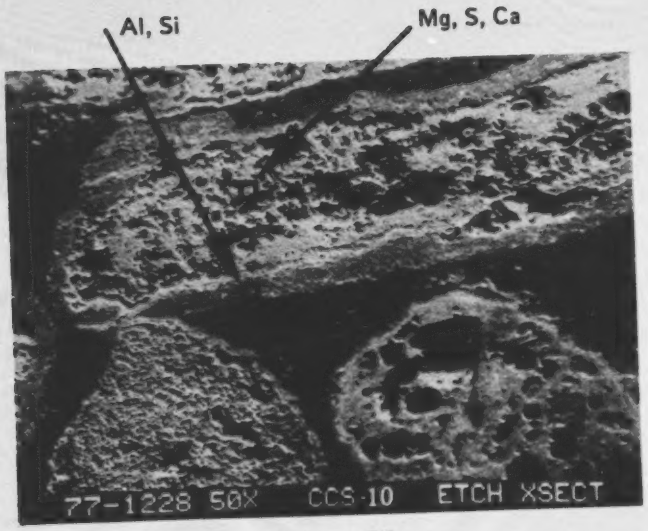

Figure 5B

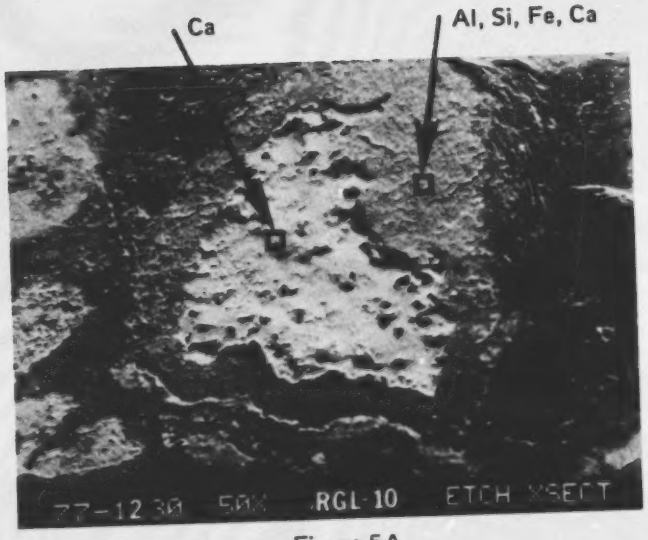

Figure 5A

Figure 6

Scanning electron micrographs and x-ray maps for Exxon samples 30.1, 30.2, and 32.0.

A. 50-diameter view of cross section of embedded 30.2 granule. Superimposed trace shows relative concentration of sulfur in the sample along the line shown.
B. 50-diameter sulfur-atom x-ray map of the view shown in Figure 6A. White dots show concentrations of sulfur in the cross section.
C. 30-diameter view of the cross sections of embedded 32.0 granules.
D. 30-diameter sulfur-atom x-ray map of the view shown in Figure 6C.
E. 75-diameter view of the cross section of an embedded 30.1 granule. Edge of granule is at left.
F. 75-diameter sulfur-atom x-ray map of the view shown in Figure 6E

Figure 6A

Figure 6B

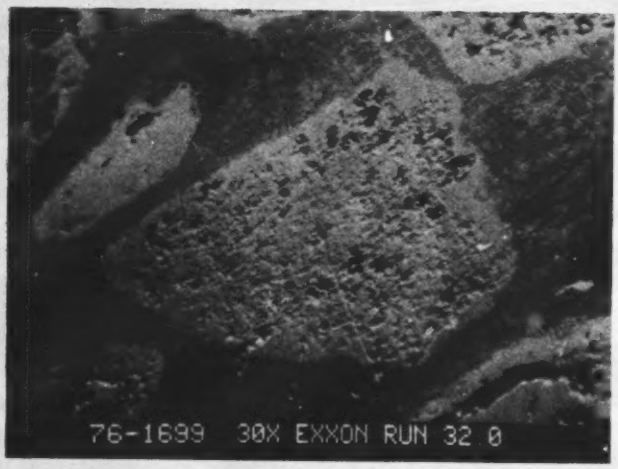

Figure 6C

Figure 6D

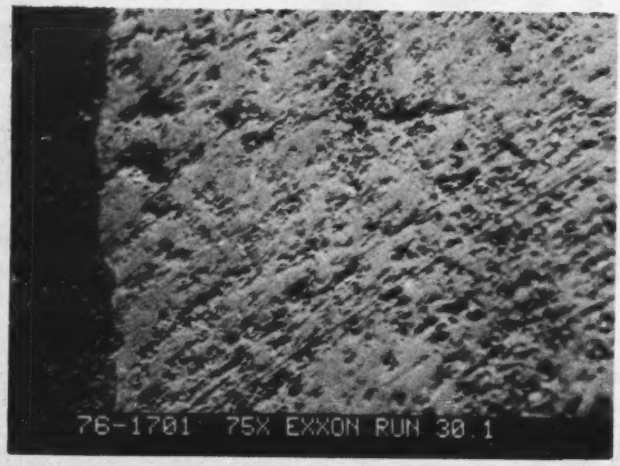

Figure 6E

Figure 6F

CPC 20" LP BED MATERIAL

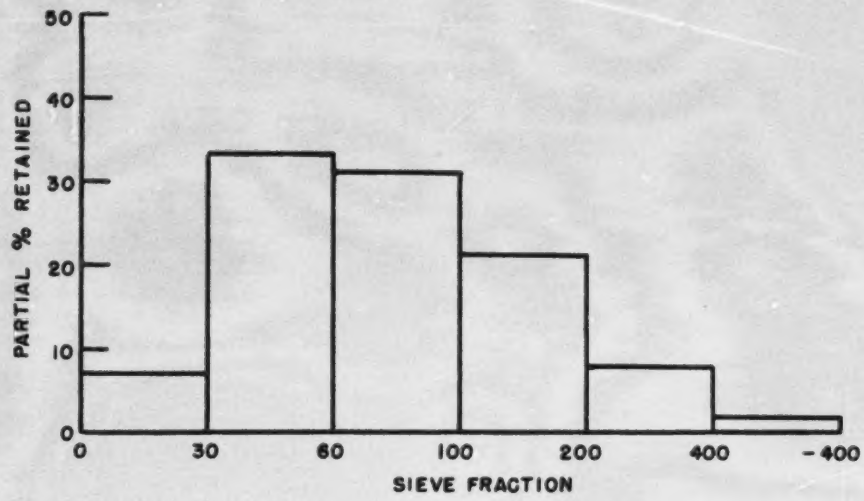

CPC 20" LP 2nd STAGE ASH

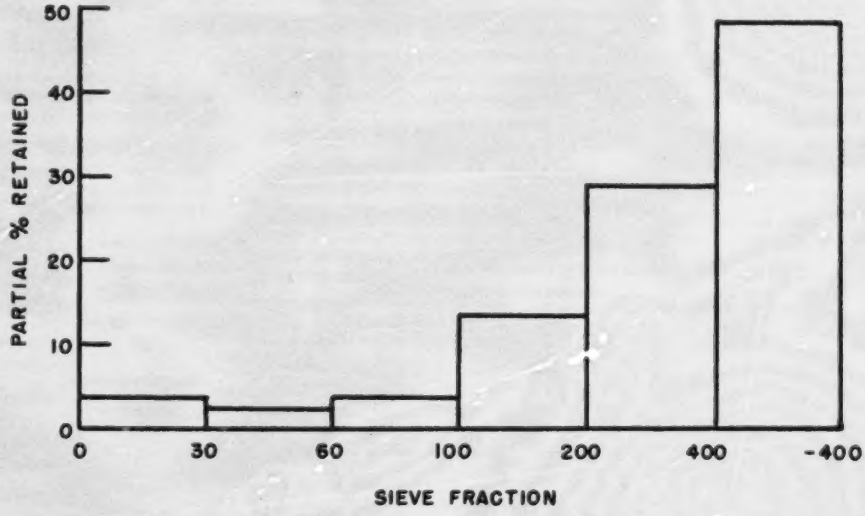

FIGURE 7

ARGONNE E-11576

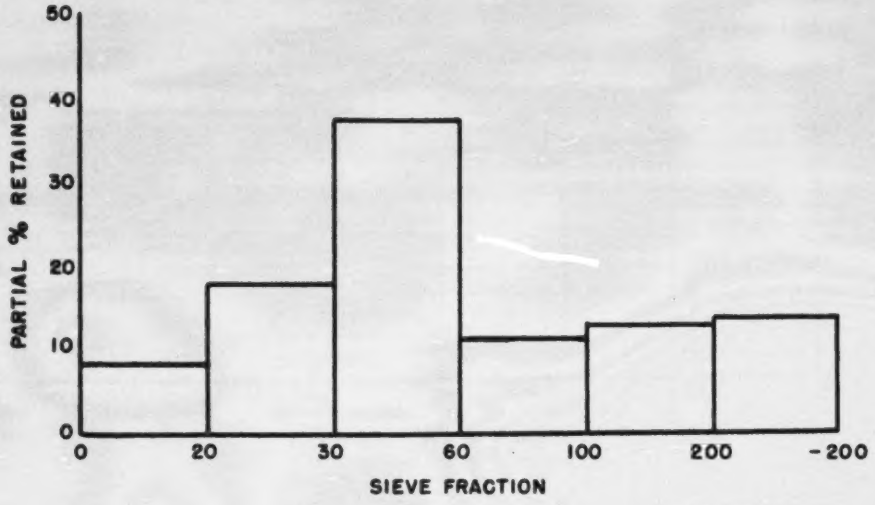

ARGONNE E-11624

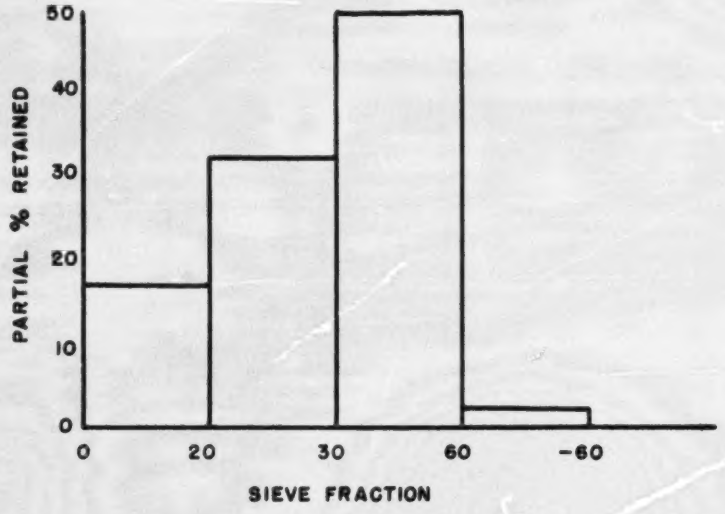

FIGURE 8

ARGONNE LST-I

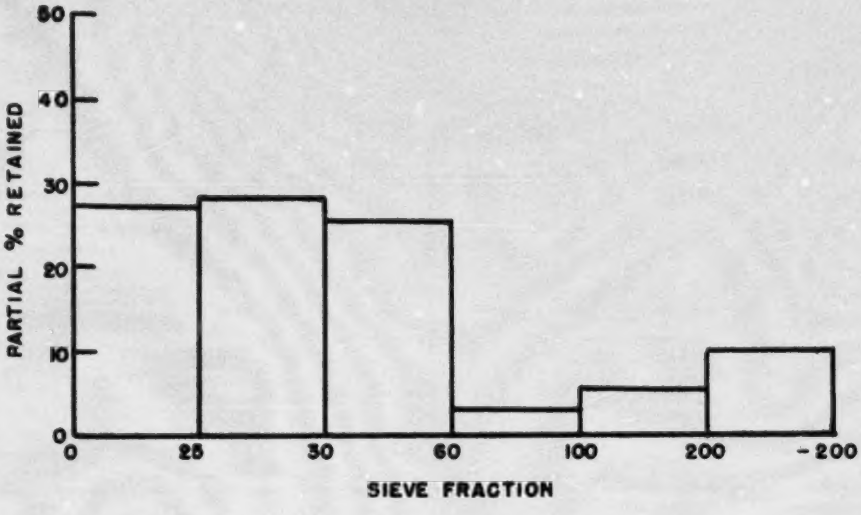

ARGONNE LST-4

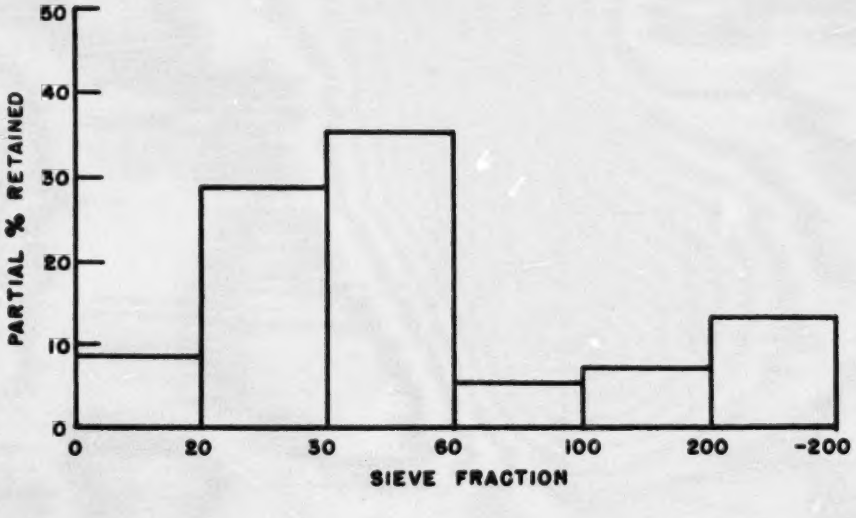

FIGURE 9

ARGONNE CCS-10

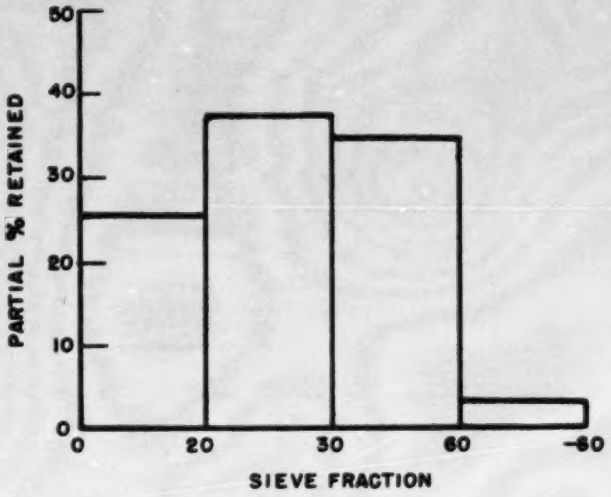

ARGONNE RGL-10

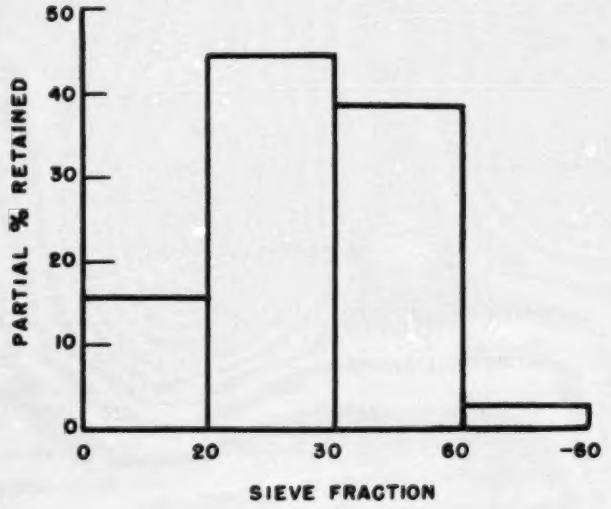

FIGURE 10

EXXON 30.1

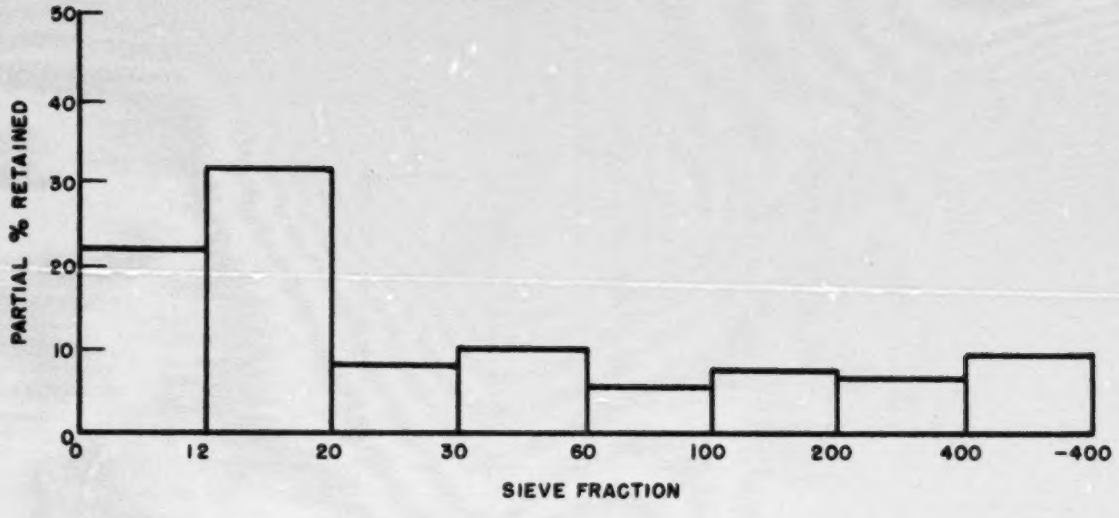

EXXON 32

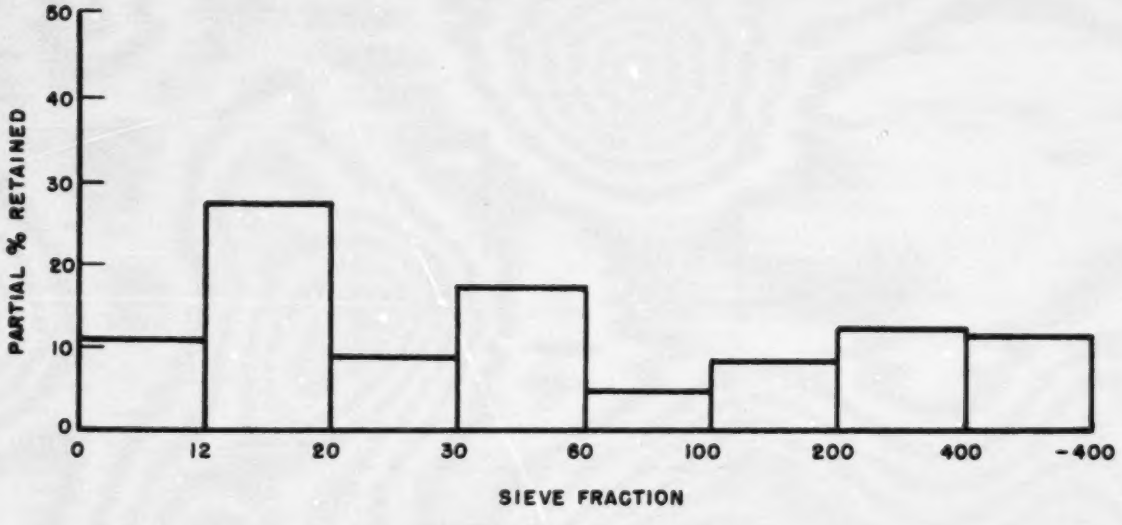

FIGURE 11

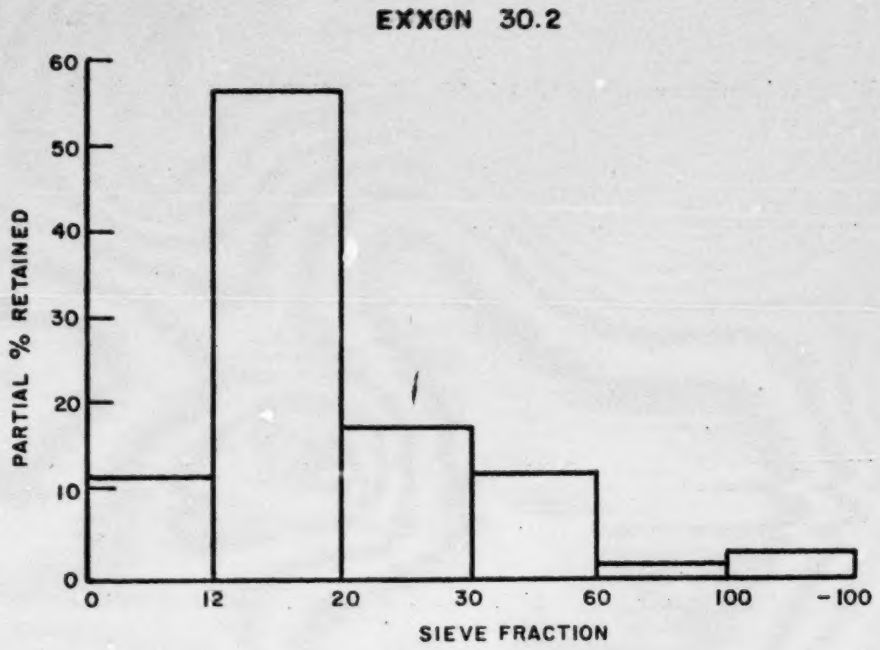
EXXON 30.2
PARTIAL % RETAINED
60
50
40
30
20
10
0
0
12
20
30
60
100
-100
SIEVE FRACTION

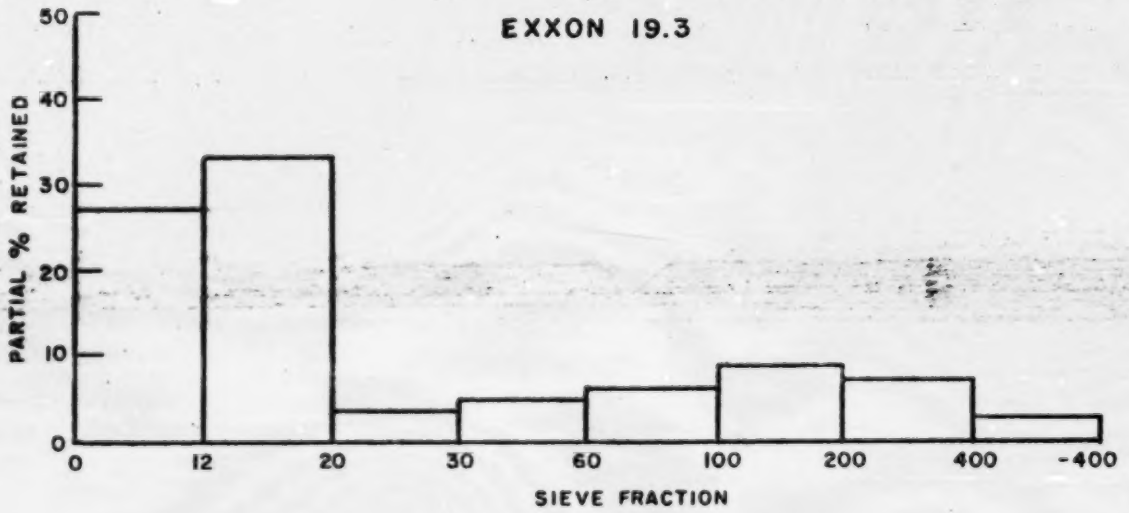
EXXON 19.3
PARTIAL % RETAINED
50
40
30
20
10
0
0
12
20
30
60
100
200
400
-400
SIEVE FRACTION

FIGURE 12